Global Design Optimization of Microwave Circuits Using Response Feature Inverse Surrogates

Anna Pietrenko-Dabrowska[1[0000-0003-2319-6782]], Slawomir Koziel[1,2[0000-0002-9063-2647]], and Leifur Leifsson[3[0000-0001-5134-870X]]

[1] Faculty of Electronics Telecommunications and Informatics, Gdansk University of Technology, Narutowicza 11/12, 80-233 Gdansk, Poland
anna.dabrowska@pg.edu.pl
[2] Engineering Optimization & Modeling Center, Department of Engineering, Reykjavík University, Menntavegur 1, 102 Reykjavík, Iceland
koziel@ru.is
[3] School of Aeronautics and Astronautics, Purdue University, West Lafayette, IN 47907, USA
leifur@purdue.edu

Abstract. Modern microwave design has become heavily reliant on full-wave electromagnetic (EM) simulation tools, which are necessary for accurate evaluation of microwave components. Consequently, it is also indispensable for their development, especially the adjustment of geometry parameters, oriented towards performance improvement. However, EM-driven optimization procedures incur considerable computational expenses, which may become impractical even in the case of local tuning, and prohibitive whenever global search is vital (e.g., multi-model tasks, simulation-based miniaturization, circuit re-design within extended ranges of operating frequencies). This work presents a novel approach to a computationally-efficient globalized parameter tuning of microwave components. Our framework employs the response feature technology, along with the inverse surrogate models. The latter permit low-cost exploration of the parameter space, and identification of the most advantageous regions that contain designs featuring performance parameters sufficiently close to the assumed target. The initial parameter vectors rendered in such a way undergo then local, gradient-based tuning. The incorporation of response features allows for constructing the inverse model using small training data sets due to simple (weakly-nonlinear) relationships between the operating parameters and dimensions of the circuit under design. Global optimization of the two microstrip components (a coupler and a power divider) is carried out for the sake of verification. The results demonstrate global search capability, excellent success rate, as well as remarkable efficiency with the average optimization cost of about a hundred of EM simulations of the circuit necessary to conclude the search process.

Keywords: Microwave design, global optimization, surrogate modeling, surrogate-assisted design, inverse models, response features.

ICCS Camera Ready Version 2022
To cite this paper please use the final published version:
DOI: 10.1007/978-3-031-08757-8_22

1 Introduction

Over the years, microwave devices become increasingly complex [1], [2], which is mainly caused by stringent performance requirements imposed thereon [3]-[5]. Another reason is miniaturization [6], which requires the employment of transmission line (TL) meandering [7] or compact microwave resonant cells (CMRCs) [8], leading to densely arranged layouts [9]. Reliable evaluation of such circuits is only possible using full-wave EM analysis. Furthermore, achieving top electrical performance requires careful tuning of all system parameters. Unfortunately, EM-driven optimization is computationally expensive, even in the case of local search. Meanwhile, in a number of situations (multimodal problems [10], multi-objective design [11], unavailability of reasonable initial designs [12]), global optimization is required, the cost of which is considerably higher.

Nowadays, global search has been dominated by nature-inspired methods [13]-[15], which come in many variations [16]-[21]. The operating principles of these methods are rooted in relaying information between the sets (populations) of competing solutions, arranged by partially stochastic operators [13]-[17]. Nature-inspired algorithms are easy to apply and handle but their computational complexity is high, with a one-time optimization run involving as many as hundreds and thousands of objective function evaluations. Consequently, practical application of nature-inspired method in high-frequency design requires utilization of acceleration techniques, the most popular of which is surrogate modeling [22], [23]. Some of specific modeling techniques being in use in this context include kriging [24], Gaussian process regression [25], and neural networks [26].

Despite its advantages, surrogate-assisted nature-inspired global search has some limitations, the most serious of which is caused by the curse of dimensionality. As far as microwave design is concerned, yet another difficulty poses high nonlinearity of frequency characteristics. Both factors make a construction of reliable surrogates difficult. In practice, only relatively simple components parameterized using a few variables can be efficiently handled [27], [28]. A recent performance-driven modeling [29], [30] can somewhat mitigate this issue by confining the modeling process to a region containing designs of superior quality w.r.t. to the performance figures of choice [29]. This concept can be generalized to variable-resolution setup [31]. Another expedient strategy is the response feature technology [32], where the design process is reformulated in terms of appositely defined characteristics points [33]. This technology capitalizes on close-to-linear relationships between the feature coordinates and designable parameters of the system at hand [34].

In this paper, we propose a novel technique for globalized parameter tuning of passive microwave devices. Our methodology is based on inverse regression surrogates, established at the tier of response features of the component under design. The surrogates allow for low-cost and rapid exploration of the parameter space, and to identify the most encouraging regions thereof. The design found with the aid of the regression model is further enhanced using the conventional gradient-based procedure. The proposed framework has been validated using two microstrip devices, and its global search capability has been demonstrated along with the low execution cost of a few dozens of EM analyses of the structure under design. Extensive benchmarking also corroborates superiority over nature-inspired optimization, as well as multiple-start gradient search.

ICCS Camera Ready Version 2022
To cite this paper please use the final published version:
DOI: 10.1007/978-3-031-08757-8_22

2 Global Design by Response-Feature Inverse Surrogates

This section outlines the proposed global optimization procedure, which employs response-feature surrogates for fast detection of the part of the design space where high-quality designs likely reside, and to render satisfactory starting points for local fine-tuning. The section begins by formulating the optimization task (Section 2.1). Section 2.2 recalls response features methodology. Global search and local tuning stages are delineated in Sections 2.3 and 2.4, respectively. Section 2.5 briefly summarizes the proposed optimization technique.

2.1 Simulation-Based Optimization. Problem Formulation

For quantifying of the performance of the microwave component under design, we adopt a merit function U. The optimization task is formulated as

$$\boldsymbol{x}^* = \arg\min_{\boldsymbol{x}} U(\boldsymbol{x}, \boldsymbol{F}_t) \quad (1)$$

where $\boldsymbol{F}_t = [F_{t.1} \ \ldots \ F_{t.K}]^T$ refers to a target vector whose entries are device operating parameters (such as operating frequencies or power split), whereas $\boldsymbol{x}$ denotes a design parameters vector (typically, circuit dimensions). The function U is evaluated based on EM-simulated characteristics of a given structure, typically, scattering parameters $S_{kl}(\boldsymbol{x},f)$, with k and l being the circuit ports, and f denoting the frequency.

2.2 Response Features for Design Assessment

Global optimization may be indispensable in the absence of a quality initial design or when given optimization task is multimodal. Yet, due to highly nonlinear relationships between the component characteristics and both design variables and frequency, as well as dimensionality issues, global search is burdensome. Moreover, finding a globally optimal design when using simulation-driven procedures is usually uneconomic. This is especially the case for nature-inspired algorithms, the cost of which may reach up to several thousands of EM-analyses of the considered component. Surrogate-based optimization of microwave passives is also encumbered by the aforementioned issues. This makes construction of reliable surrogates for structures described by an extended number of design variables and, at the same time, within sufficiently broad parameter ranges virtually unrealizable using conventional metamodeling techniques.

One of the available approaches for circumventing the aforementioned difficulties is response features technology [32]. The said technique operates at the tier of the characteristic points of the circuit response (in contrast to traditional procedures which handle the response in its entirety). The rationale behind adopting this strategy is the fact that the relationship between the features and design variables is nonlinear to a considerably smaller degree than that of the entire characteristic, as shown in Fig. 1 for an example microwave component (miniaturized compact rat-race coupler). The feature points are defined with regard to the particular formulation of the optimization task at hand, as well as the actual shape of the circuit response. Various definitions include: frequency and level coordinates of the resonances [34], or points that delineate a bandwidth [35].

ICCS Camera Ready Version 2022
To cite this paper please use the final published version:
DOI: 10.1007/978-3-031-08757-8_22

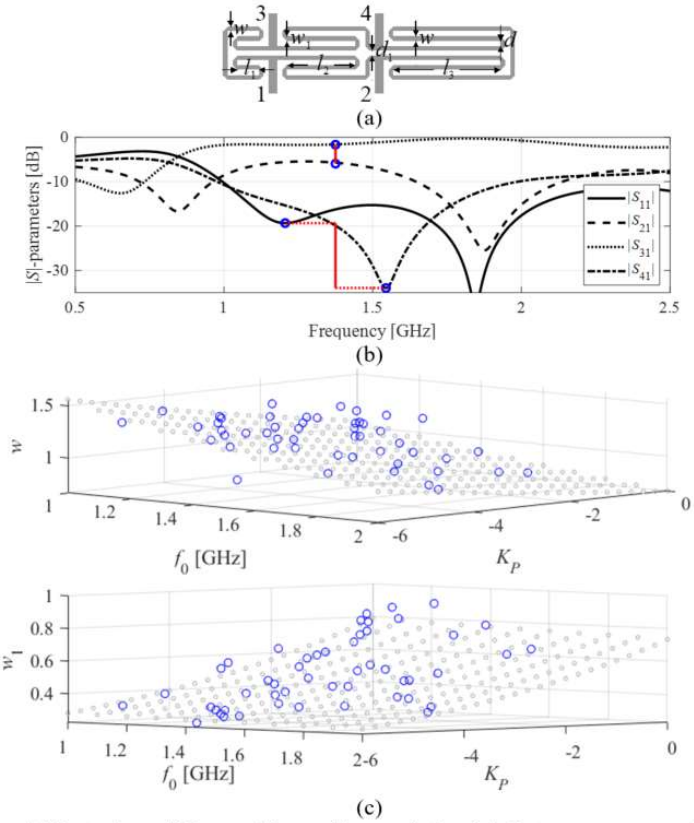

Fig. 1. Visual illustration of the weakly-nonlinear relationship between response features and geometry parameters of a circuit: a) an example structure (compact rat-race coupler), b) characteristic points corresponding to the minima of $|S_{11}|$ and $|S_{41}|$, and power split ratio K_P (marked with circles); the vertical line indicates the approximate circuit operating frequency f_0 (assessed as the minima average); c) relationship between the f_0 and K_P and the selected design variables; the designs are marked with the circles, whereas the regression model is shown with gray points.

In Fig. 1(b), the operating frequency of the circuit (denoted as f_0) is roughly estimated as the midpoint between the minima of the matching and isolation characteristic, and the power split is assessed as $K_P = |S_{21}(f_0)| - |S_{31}(f_0)|$. Clearly, for certain designs, some of (or even all) the feature points may not be discernible. Figure 1(c) depicts the relationship between f_0 and K_P and two design variables of the coupler of Fig. 1(a). The circuit designs are shown against the inverse regression model $\alpha_0 + \alpha_1 \exp(\alpha_2 f_0 + \alpha_3 K_P)$ representing the trends between the circuit operating and geometry parameters. This form of a regression model is sufficient to describe weakly nonlinear dependence of the device dimensions on its operating parameters, which characterizes many real-world components and devices.

ICCS Camera Ready Version 2022
To cite this paper please use the final published version:
DOI: 10.1007/978-3-031-08757-8_22

Table 1. Global optimization using inverse feature-based surrogates: Notation

Notation	Description
$\boldsymbol{F}(\boldsymbol{x}) = [F_1(\boldsymbol{x}) \ldots F_K(\boldsymbol{x})]^T$	Operating parameter vector at the design $\boldsymbol{x}$ (estimated based on response features extracted from EM-simulated response); if some features are indiscernible and the parameters cannot be assessed: $\boldsymbol{F}(\boldsymbol{x}) = [0 \ldots 0]^T$
$\boldsymbol{L}(\boldsymbol{x}) = [l_1(\boldsymbol{x}) \ldots l_K(\boldsymbol{x})]^T$	Auxiliary vector whose entries are design quality coefficients (corresponding to those of $\boldsymbol{F}(\boldsymbol{x})$); if some elements of $\boldsymbol{L}(\boldsymbol{x})$ cannot be derived: $\boldsymbol{L}(\boldsymbol{x}) = [0 \ldots 0]^T$
$D(\boldsymbol{F},\boldsymbol{F}_t)$	Distance function that measures the misalignment between the target vector $\boldsymbol{F}_t$ and the current one $\boldsymbol{F}$; here: $D(\boldsymbol{F},\boldsymbol{F}_t) = \|\boldsymbol{F} - \boldsymbol{F}_t\|$ (i.e., we use L_2-norm-based distance)
D_{accept}	Termination parameter (user-defined) of the global search stage: if $D(\boldsymbol{F}, \boldsymbol{F}_t) \leq D_{accept}$ the design $\boldsymbol{x}$ is acceptably close to the target $\boldsymbol{F}_t$

2.3 Global Search Stage Using Inverse Models

In the presented approach, parameters of the inverse regression model are estimated based on randomly acquired observables. As the observable quality with respect to the target performance requirements is not known beforehand, we need a measure to assess it and to decide whether a particular observable is to be accepted or not. Here, this quality is quantified with the use of the response features derived from the frequency characteristics, which are subsequently compared with the assumed targets. The accepted observables are then utilized to build an inverse regression surrogate, which is exploited to delimit the promising region of the design space, and also to render infill points for the metamodel refinement. In each iteration, a single infill point is reinserted to the observable set replacing that of the poorest quality.

The adopted notation is provided in Table 1. Some additional clarification is required on the vector $\boldsymbol{L}(\boldsymbol{x})$: its entries are the design quality coefficients, definition of which is problem-specific. If the design process aims at minimizing the levels of the reflection and isolation characteristics at the operating frequency, the respective coefficient l_k may be defined as the mean of $|S_{11}|$ and $|S_{41}|$ at the said minima. If, however, power split ratio is of interest, the correspondent l_k may be a discrepancy between the actual power split and the target one. In this work, the coefficients l_k are normalized, i.e., $0 \leq l_k \leq 1$: we have $l_k = 0$ for the best design, and $l_k = 1$ for the design of the lowest quality

The essential steps of the discussed global optimization procedure include: rendering observables intertwined by the construction and refinement of the inverse surrogate, followed by rendering a candidate design, and concluded by its tuning in the case it is close enough to the target. The random observables, i.e., parameter vectors $\boldsymbol{x}^{(j)} = [x_1^{(j)} \ldots x_n^{(j)}]^T$, $j = 1, \ldots, N$, are uniformly spaced within the box-constrained design space X, delimited by the lower and upper variable boundaries. The observable generation stops when N designs of $\|\boldsymbol{F}(\boldsymbol{x}^{(j)})\| > 0$, $j = 1, \ldots, N$, have been gathered. The triplets $\{\boldsymbol{F}(\boldsymbol{x}^{(j)}), \boldsymbol{L}(\boldsymbol{x}^{(j)}), \boldsymbol{x}^{(j)}\}_{j=1,\ldots,N}$, constitute a training data for an inverse regressive metamodel $r_I(\boldsymbol{F})$, which assesses the trend between circuit operating parameters and dimensions. Once the inverse surrogate is constructed, it is utilized for prediction of the candidate design $\boldsymbol{x}_{tmp} = r_I(\boldsymbol{F}_t)$ for a given operating parameter vector $\boldsymbol{F}_t$. If the two following conditions

ICCS Camera Ready Version 2022
To cite this paper please use the final published version:
DOI: 10.1007/978-3-031-08757-8_22

are satisfied: $||\boldsymbol{F}(\boldsymbol{x}_{tmp})|| > 0$ and $D(\boldsymbol{F}(\boldsymbol{x}_{tmp}),\boldsymbol{F}_t) < \max\{j = 1, \ldots, N : D(\boldsymbol{F}(\boldsymbol{x}^{(j)}),\boldsymbol{F}_t)\}$, the design $\boldsymbol{x}_{tmp}$ substitutes that of the largest distance $D(\boldsymbol{F}(\boldsymbol{x}^{(j)}),\boldsymbol{F}_t)\}$. Ultimately, the inverse surrogate is reset with a new training set.

The inverse model (re)construction and design prediction are reprised until a design sufficiently close to the assumed target is detected, i.e., the design for which $D(\boldsymbol{F}(\boldsymbol{x}_{tmp}),\boldsymbol{F}_t) < D_{\max}$, where $D_{\max}$ denotes an acceptance threshold (set by the user). This design is subsequently refined in the local tuning stage. In the case such a design has not been reached, the procedure is executed until the assumed computational budget has ran out, then, the best design is returned. Figure 2 explains graphically the aforementioned concepts: starting from observable generation, through inverse model construction and refinement, until local tuning of the globally optimal design. Note that Figs. 2 (b)-(d) show the procedure for a single variable x, which, in fact, is carried out for all the parameters concurrently.

The analytical form of the inverse surrogate $r_I(\boldsymbol{F})$ does not need to be intricate, as the relation between operating parameters and circuit dimensions is weakly nonlinear. Still, it is essential to ensure a sufficient flexibility, since this dependence may in some cases be inversely proportional. Therefore, we adopt a regression model of the form:

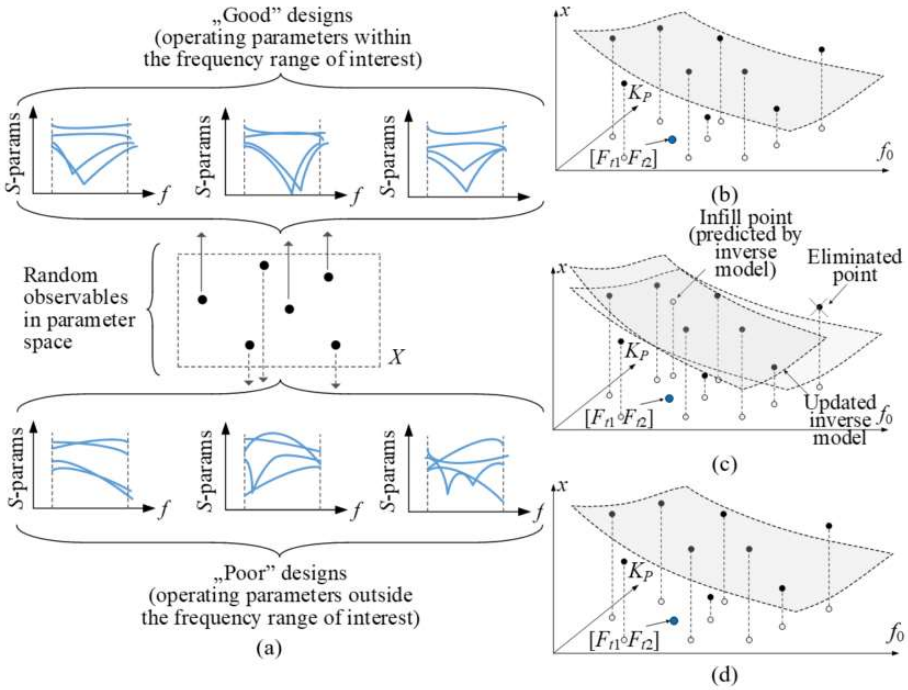

Fig. 2. Major stages of the presented global optimization framework: (a) selection of high-quality observables, (b) two-dimensional objective space: observables (•) and their projections onto the f_0-K_P plane, the initial inverse surrogate (gray surface); the target vector of operating parameters (blue circle); (c) first iteration: the infill point rendered by r_I (gray circle) substitutes the poorest observable and the model is reset; (d) final iteration: the observables are focused in the proximity of the target operating parameters and r_I predicts the design close enough to the target.

ICCS Camera Ready Version 2022
To cite this paper please use the final published version:
DOI: 10.1007/978-3-031-08757-8_22

$$\boldsymbol{r}_I(\boldsymbol{F}) = \boldsymbol{r}_I\left(\begin{bmatrix} f_1 \\ \dots \\ f_K \end{bmatrix}\right) = \begin{bmatrix} r_{I.1}(\boldsymbol{F}) \\ \cdots \\ r_{I.n}(\boldsymbol{F}) \end{bmatrix} = \begin{bmatrix} p_{1.0} + p_{1.1} e^{\sum_{k=1}^{K} p_{1.k+1} f_k} \\ \cdots \\ p_{n.0} + p_{n.1} e^{\sum_{k=1}^{K} p_{n.k+1} f_k} \end{bmatrix} \quad (2)$$

In order to identify the surrogate $r_I(\boldsymbol{F})$, one needs to solve

$$\left[p_{j.0}\ p_{j.1} \cdots p_{j.K+1}\right] = \arg \min_{[b_0\ b_1 \dots b_{K+1}]} \sum_{k=1}^{N} w_k \left[r_{I.j}\left(\boldsymbol{F}(\boldsymbol{x}^{(k)})\right) - x_j^{(k)}\right]^2,\ j = 1,\ \dots, n \quad (3)$$

using the triplets $\{\boldsymbol{F}(\boldsymbol{x}^{(j)}), \boldsymbol{L}(\boldsymbol{x}^{(j)}), \boldsymbol{x}^{(j)}\}_{j=1,\dots,N}$, as training data samples. The weights $w_k = [1 - \max\{l_1(\boldsymbol{x}^{(j)}),\dots, l_k(\boldsymbol{x}^{(j)})\}]^2$, $k = 1, \dots, N$, are to ensure that the high-quality observables influence r_I in a more significant manner.

2.4 Local Tuning

The design $\boldsymbol{x}^{(0)}$ rendered by the global optimization procedure of Section 2.3 satisfies the condition $D(\boldsymbol{F}(\boldsymbol{x}^{(0)}),\boldsymbol{F}_t) \leq D_{accept}$, where the value of the threshold D_{accept} is set so as to ensure that the operating parameters at $\boldsymbol{x}^{(0)}$ are in a sufficient proximity to $\boldsymbol{F}_t$. This is to enable reaching the target through a local search procedure. Here, we exploit the trust-region (TR) optimization algorithm with numerical derivatives [36], which renders a series designs $\boldsymbol{x}^{(i)}$, $i = 0, 1, \dots$ that approximate the optimal solution $\boldsymbol{x}^*$, by solving

$$\boldsymbol{x}^{(i+1)} = \arg \min_{\boldsymbol{x};\ -\boldsymbol{d}^{(i)} \leq \boldsymbol{x} - \boldsymbol{x}^{(i)} \leq \boldsymbol{d}^{(i)}} U_L(\boldsymbol{x}, \boldsymbol{F}_t) \quad (4)$$

within the trust region of the perimeter $\boldsymbol{d}^{(i)}$. The TR region size is determined according to the routine setup of the TR algorithm [36]. The merit function U_L (4) is of the same form as U, yet, it is evaluated with the use of the first-order Taylor model $\boldsymbol{G}^{(i)}(\boldsymbol{x},f)$ of the circuit responses at the vector $\boldsymbol{x}^{(i)}$: $\boldsymbol{G}^{(i)}(\boldsymbol{x},f) = S_{kl}(\boldsymbol{x}^{(i)},f) + \nabla_{Skl}(\boldsymbol{x}^{(i)},f)\cdot(\boldsymbol{x} - \boldsymbol{x}^{(i)})$. The linear model is defined for the scattering parameter S_{kl}, with the gradients estimated through finite differentiation (FD). This adds n EM simulations for each iteration to the overall optimization cost. The local search terminates if $\|\boldsymbol{x}^{(i+1)} - \boldsymbol{x}^{(i)}\| < \varepsilon$ (convergence in argument), or the TR size has shrunk below ε, i.e., $\|\boldsymbol{d}^{(i)}\| < \varepsilon$. In this work, we employ $\varepsilon = 10^{-3}$. For computational efficiency, when approaching convergence (i.e., for $\|\boldsymbol{x}^{(i+1)} - \boldsymbol{x}^{(i)}\| < 10\varepsilon$) the rank-one Broyden formula [36] takes the place of FD for gradient evaluation.

2.5 Algorithm Summary

This section summarizes the proposed global search procedure with feature-based inverse surrogates, the main stages of which include the global exploration stage described in Section 2.3, in which the starting point $\boldsymbol{x}^{(0)}$ is found, and the local refinement procedure (Section 2.4) that yields the design $\boldsymbol{x}^*$ using the trust-region algorithm as a search engine. The control parameters of our technique include: the number N of the observables required for inverse surrogate construction and the threshold D_{accept}. Typically, N of the same order as parameter space dimensionality is a reasonable choice; yet, N should also account for the number of design objectives so as to adequately represent the curvature of the set comprising high-quality designs. The purpose of the second parameter D_{accept} is to ensure attainability of the assumed targets through a local search.

ICCS Camera Ready Version 2022
To cite this paper please use the final published version:
DOI: 10.1007/978-3-031-08757-8_22

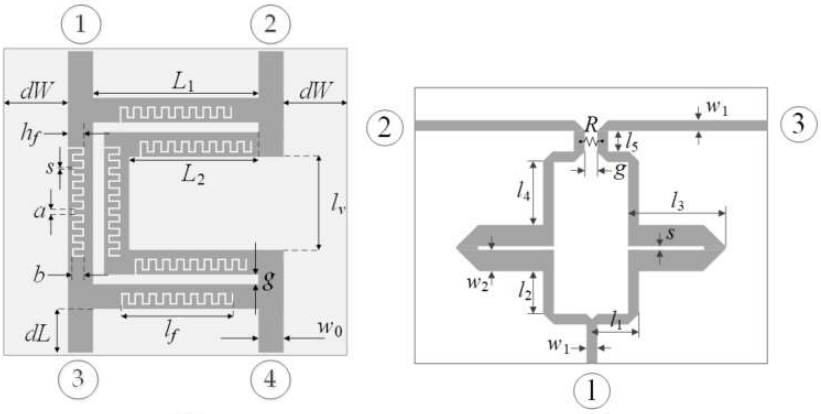

Fig. 3. Verification case strictures: (a) rat-race coupler with defected microstrip structure (RRC) [37], and (b) dual-band power divider (PD), with the lumped resistor marked as R [38].

If the operating parameters are circuit operating frequency (or frequencies), which is often the case, D_{accept} should be equal to around 50 percent of the target bandwidth. The parameters $N_{max.k}$, k = 1, 2, 3, (maximal number of EM analyses for initial sampling, global and local search phase, respectively) serve to define the computational budget. Their values should give enough room for the algorithm to converge with a sufficient accuracy, typically it suffices if $N_{max.1}$ and $N_{max.2}$ equal around $10n$, and $N_{max.3}$ is around five times higher.

3 Verification Experiments

This section reports the results of a numerical verification of the proposed global optimization procedure. The performance of our methodology is demonstrated using a miniaturized coupler and a dual-band power divider. The obtained results are benchmarked against: (i) local optimization starting from multiple random initial deigns (to justify the necessity for a global search), and (ii) particle swarm optimizer (commonly choice for performing global search). The control parameters of our framework are: $N = 10$, $D_{accept} = 0.2$, $N_{max.1} = N_{max.2} = 100$, $N_{max.3} = 500$, $\varepsilon = 10^{-3}$. For the benchmark PSO procedure we have: population size 10, $\chi = 0.73$, and $c_1 = c_2 = 2.05$. We also adopt standard setup [36] of the TR algorithm.

3.1 Verification Circuits

The verification structures utilized to validate the proposed approach are shown in Fig. 3. The first circuit is a miniaturized rat-race coupler (RRC), in which a defected meander spurline inside a folded transmission line is employed [37]. RRC is fabricated on a substrate of the height h = 0.15 mm. The vector of design variables is $\boldsymbol{x} = [L_1\ b_r\ g\ h_{fr}\ s\ l_{fr}]^T$ (dimensions in mm apart from unitless relative parameters indicated with the subscript r). We also have: $L_2 = L_1 - g - w_0$, $a = (l_f - 17s)/16$, $b = (h_f - s)b_r$, $l_f = L_2\ l_{fr}$, $l_v = L_1 - 2g - 2w_0$, and $h_f = s + (w_0 - s)h_{fr}$; $dW = dL = 10$ mm. The width w_0 of input line

ICCS Camera Ready Version 2022
To cite this paper please use the final published version:
DOI: 10.1007/978-3-031-08757-8_22

is evaluated taking into account substrate permittivity ε_r to obtain 50 Ω input impedance. The lower and upper boundaries of the parameters are: $\boldsymbol{l}$ = [20.0 0.1 1.0 0.2 0.2 0.2]^T and $\boldsymbol{u}$ = [15.0 30.0 50.0 2.0 2.0 2.0]^T. The design objectives are: (i) minimization of $|S_{11}|$ and $|S_{41}|$ characteristics (matching and isolation, respectively) at the target operating frequency f_0, and (ii) obtaining equal power split $d_S(\boldsymbol{x},f_0) = |S_{21}(\boldsymbol{x},f_0)| - |S_{31}(\boldsymbol{x},f_0)|$. The merit function is formulated as

$$U(\boldsymbol{x},\boldsymbol{F}_t) = U(\boldsymbol{x},[f_0\ K_P]^T) = \max\{|S_{11}(\boldsymbol{x},f_0)|,|S_{41}(\boldsymbol{x},f_0)|\} + \beta\left[d_S(\boldsymbol{x},f_0)\right]^2 \quad (5)$$

The second component of (5) is a penalty function ensuring equal power split ratio, and β denotes the penalty factor. Two design cases have been considered: (i) f_0 = 1.5 GHz, ε_r = 2.5, and (ii) (i) f_0 = 1.2 GHz, ε_r = 4.4.

The second structure is a dual-band equal-split power divider (PD) [38], implemented on AD250 substrate of ε_r = 2.5, and h = 0.81 mm. The circuit variables are $\boldsymbol{x}$ = [l_1 l_2 l_3 l_4 l_5 s w_2]^T (all in mm); fixed dimensions: w_1 = 2.2 mm and g = 1 mm. The lower and upper parameter boundaries are: $\boldsymbol{l}$ = [10.0 1.0 10.0 0.5 1.0 0.1 1.5]^T and $\boldsymbol{u}$ = [40.0 20.0 40.0 15.0 6.0 1.5 8.0]^T, respectively. The goal is to minimize $|S_{11}|$, $|S_{22}|$, $|S_{33}|$, and $|S_{23}|$ (input matching, output matching, and isolation, respectively) at the operating frequencies $f_{0.1}$ and $f_{0.2}$. The objective function is formulated as

$$\begin{aligned} U(\boldsymbol{x},\boldsymbol{F}_t) = U(\boldsymbol{x},[f_{0.1}\ f_{0.2}]^T) = \max\{&|S_{11}(\boldsymbol{x},f_{0.1})|,|S_{22}(\boldsymbol{x},f_{0.1})|,|S_{33}(\boldsymbol{x},f_{0.1})|,\\ &|S_{23}(\boldsymbol{x},f_{0.1})|,|S_{11}(\boldsymbol{x},f_{0.2})|,|S_{22}(\boldsymbol{x},f_{0.2})|,|S_{33}\boldsymbol{x},f_{0.2})|,|S_{23}(\boldsymbol{x},f_{0.2})|\} \end{aligned} \quad (6)$$

Table 2. Optimization results for circuits of Fig. 3

Circuit	Target operating parameters	Optimization method	Proposed algorithm	PSO		TR-based local search
				50 iterations	100 iterations	
RRC	f_0 = 1.5 GHz, ε_r = 2.5	Average objective function value [dB]	–18.6	–17.6	–19.2	–1.8
		Computational cost[$]	85.5	500	1,000	77.0
		Success rate[#]	10/10	10/10	10/10	5/10
	f_0 = 1.2 GHz, ε_r = 4.4	Average objective function value [dB]	–21.5	–19.4	–22.5	7.6
		Computational cost[$]	90.2	500	1,000	83.8
		Success rate[#]	10/10	9/10	10/10	5/10
PD	f_1 = 3.0 GHz, f_2 = 4.8 GHz	Average objective function value [dB]	–33.9	–19.6	–18.8	–12.3
		Computational cost[$]	99.1	500	1,000	95.1
		Success rate[#]	10/10	8/10	9/10	2/10
	f_1 = 2.0 GHz, f_2 = 3.3 GHz	Average objective function value [dB]	–23.6	–18.8	–19.7	–20.6
		Computational cost[$]	99.2	500	1,000	93.8
		Success rate[#]	10/10	8/10	9/10	7/10

[$] The cost expressed in terms of the number of EM analyses of the circuit under design.
[#] Number of algorithm runs with operating parameters meeting the condition $D(\boldsymbol{F}(\boldsymbol{x}^*),\boldsymbol{f}_t) \le D_{accept}$.

ICCS Camera Ready Version 2022
To cite this paper please use the final published version:
DOI: 10.1007/978-3-031-08757-8_22

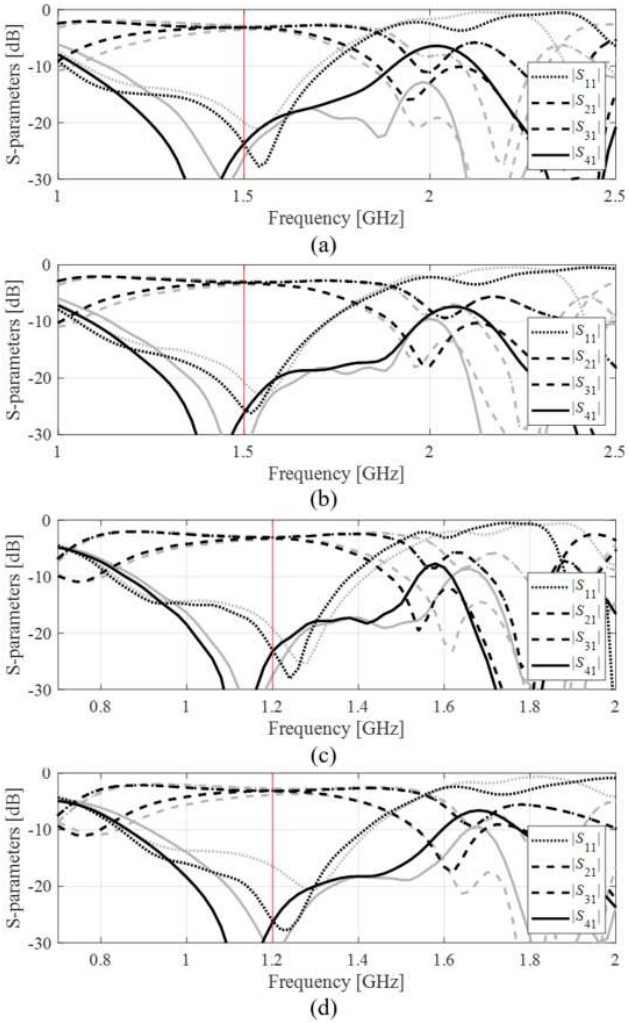

Fig. 4. Global search with inverse surrogates, S-parameters of RRC: (i) $f_0 = 1.5$ GHz, $\varepsilon_r = 2.5$ (a), (b) Designs 1 and 2, respectively, (ii) $f_0 = 1.2$ GHz, $\varepsilon_r = 4.4$: (c), (d) Designs 1 and 2, respectively. The initial design rendered within the global search stage is marked gray, the refined design is marked black. Vertical line marks the target operating frequency.

Here, the equal power split condition is enforced by the structure symmetry, thus, it does not need to be dealt with in the optimization process. The following design cases have been considered: (i) $f_{0.1} = 3.0$ GHz, $f_{0.2} = 4.8$ GHz, and (ii) $f_{0.1} = 2.0$ GHz, $f_{0.2} = 3.3$ GHz. The simulation models of both devices are realized in CST Microwave Studio, and evaluated using its transient solver.

3.2 Results

Table 2 provides the numerical results for both RRC and PD. The circuit responses at the designs optimized by the discussed global optimization framework are shown in

ICCS Camera Ready Version 2022
To cite this paper please use the final published version:
DOI: 10.1007/978-3-031-08757-8_22

Figs. 4 and 5. The main observations concerning the presented optimization strategy may be summarized as follows. Our approach exhibits a global search capability as high-grade designs have been yielded in all the ten runs of the algorithm. Moreover, Figs. 4 and 5 show that the global search stage renders high-quality designs (with the operating frequency allocated close to the target). As for the benchmark TR algorithm from random initial designs, it fails in half of the cases. Although PSO optimizer performs much better, yet, its CPU cost is considerably higher that of the proposed procedure.

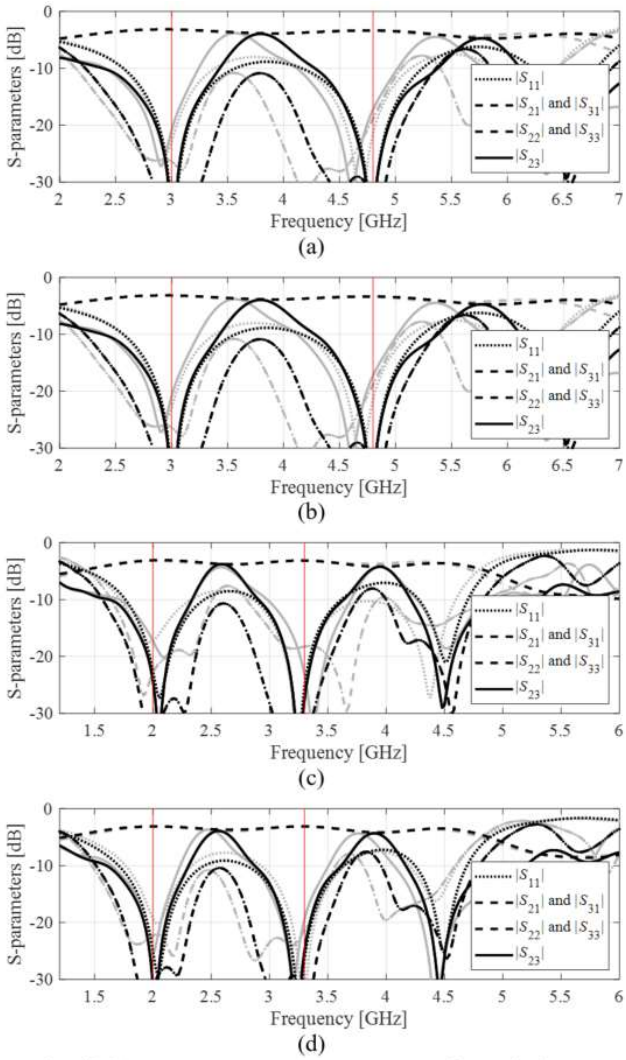

Fig. 5. Global search with inverse surrogates, S-parameters of PD: (i) $f_{0.1}$ = 3.0 GHz, $f_{0.2}$ = 4.8 GHz, (a), (b) Designs 1 and 2, respectively, (ii) $f_{0.1}$ =2.0 GHz, $f_{0.2}$ = 3.3 GHz: (c), (d) Designs 1 and 2, respectively. The initial design rendered within the global search stage is marked gray, the refined design is marked black. Vertical line marks the target operating frequency.

ICCS Camera Ready Version 2022
To cite this paper please use the final published version:
DOI: 10.1007/978-3-031-08757-8_22

As far as the design quality is concerned, for our technique, it is significantly higher than for both benchmark procedures. Moreover, our approach is virtually immune to the initial design quality, which proves its robustness. The proposed methodology is only somewhat more expensive than gradient-based local search (of around ten percent). This efficiency is due to the employment of feature-based inverse surrogates, particularly, constructing the metamodel over low-dimensional objective space. The aforementioned advantages make the presented technique a low-cost alternative to mainstream global optimization methods.

4 Conclusions

The paper presented a low-cost procedure for global design optimization of microwave passives. The key concept of our framework is the employment of response feature inverse regression surrogates. The computational efficiency of the proposed technique capitalizes on weakly nonlinear relationship between the response features and geometry parameters of the system at hand, which allows for rendering the inverse model using only a handful of pre-selected random observables. The proposed procedure has been validated using a miniaturized rat-race coupler, and a dual-band power divider. The CPU cost of our framework is only slightly higher than the cost of a local search and significantly lower than that of a PSO optimization algorithm.

Acknowledgement

The authors would like to thank Dassault Systemes, France, for making CST Microwave Studio available. This work is partially supported by the Icelandic Centre for Research (RANNIS) Grant 206606 and by National Science Centre of Poland Grant 2020/37/B/ST7/01448.

References

1. Ma, P., Wei, B., Hong, J., Xu, Z., Cao, B., Jiang, L.: A design method of multimode multiband bandpass filters. IEEE Trans. Microwave Theory Techn., **66**(6), pp. 2791–2799 (2018)
2. Yang, Q., Jiao, Y., Zhang, Z.: Compact multiband bandpass filter using low-pass filter combined with open stub-loaded shorted stub. IEEE Trans. Microwave Theory Techn., **66**(4), pp. 1926–1938 (2018)
3. Hagag, M. F., Zhang, R., Peroulis, D.: High-performance tunable narrowband SIW cavity-based quadrature hybrid coupler. IEEE Microwave Wireless Comp. Lett., **29**(1), pp. 41–43 (2019)
4. Gómez-García, R., Rosario-De Jesus, J., Psychogiou, D.: Multi-band bandpass and bandstop RF filtering couplers with dynamically-controlled bands. IEEE Access, **6**, pp. 32321–32327 (2018)
5. Zhang, R., Peroulis, D.: Mixed lumped and distributed circuits in wideband bandpass filter application for spurious-response suppression. IEEE Microwave Wireless Comp. Lett., **28**(11), pp. 978–980 (2018)

ICCS Camera Ready Version 2022
To cite this paper please use the final published version:
DOI: 10.1007/978-3-031-08757-8_22

6. Sheikhi, A., Alipour, A., Mir, A.: Design and fabrication of an ultra-wide stopband compact bandpass filter. IEEE Transactions Circuits Syst. II, **67**(2), pp. 265–269 (2020)
7. Firmansyah, T., Alaydrus, M., Wahyu, Y., Rahardjo, E. T., Wibisono, G.: A highly independent multiband bandpass filter using a multi-coupled line stub-SIR with folding structure. IEEE Access, **8**, pp. 83009–83026 (2020)
8. Chen, S., Guo, M., Xu, K., Zhao, P., Dong, L., Wang, G.: A frequency synthesizer based microwave permittivity sensor using CMRC structure. IEEE Access, **6**, pp. 8556–8563 (2018)
9. Chi, J. G. Kim, Y. J.: A compact wideband millimeter-wave quadrature hybrid coupler using artificial transmission lines on a glass substrate. IEEE Microwave Wireless Comp. Lett., **30**(11), pp. 1037–1040 (2020)
10. Koziel, S., Abdullah, M.: Machine-learning-powered EM-based framework for efficient and reliable design of low scattering metasurfaces. IEEE Trans. Microwave Theory Techn. **69**(4), pp. 2028–2041 (2021)
11. Rayas-Sanchez, J. E., Koziel, S., Bandler, J. W.: Advanced RF and microwave design optimization: a journey and a vision of future trends. IEEE J. Microwaves, **1**(1), pp. 481–493 (2021)
12. Jin, H., Zhou, Y., Huang, Y. M., Ding, S., Wu, K.: Miniaturized broadband coupler made of slow-wave half-mode substrate integrated waveguide. IEEE Microwave Wireless Comp. Lett., **27**(2), pp. 132–134 (2017)
13. Li, X., Luk, K. M.: The grey wolf optimizer and its applications in electromagnetics. IEEE Trans. Ant. Prop., **68**(3), pp. 2186–2197 (2020)
14. Luo, X., Yang, B., Qian, H. J.: Adaptive synthesis for resonator-coupled filters based on particle swarm optimization. IEEE Trans. Microwave Theory Techn., **67**(2), pp. 712–725 (2019)
15. Majumder, A., Chatterjee, S., Chatterjee, S., Sinha Chaudhari, S., Poddar, D. R.: Optimization of small-signal model of GaN HEMT by using evolutionary algorithms. IEEE Microwave Wireless Comp. Lett., **27**(4), pp. 362–364 (2017)
16. Ding, D., Zhang, Q., Xia, J., Zhou, A., Yang, L.: Wiggly parallel-coupled line design by using multiobjective evolutionay algorithm. IEEE Microwave Wireless Comp. Lett., **28**(8), pp. 648–650 (2018)
17. Zhu. D. Z., Werner, P. L., Werner, D. H.: Design and optimization of 3-D frequency-selective surfaces based on a multiobjective lazy ant colony optimization algorithm. IEEE Trans. Ant. Propag., **65**(12), pp. 7137–7149 (2017)
18. Greda, L. A., Winterstein, A., Lemes, D. L., Heckler, M. V. T.: Beamsteering and beamshaping using a linear antenna array based on particle swarm optimization. IEEE Access, **7**, pp. 141562–141573 (2019)
19. Cui, C., Jiao, Y., Zhang, L.: Synthesis of some low sidelobe linear arrays using hybrid differential evolution algorithm integrated with convex programming. IEEE Ant. Wireless Propag. Lett., **16**, pp. 2444–2448 (2017)
20. Baumgartner, P., Baurnfeind, T., Biro, O., Hackl, A., Magele, C., Renhart, W., Torchio, R.: Multi-objective optimization of Yagi-Uda antenna applying enhanced firefly algorithm with adaptive cost function. IEEE Trans. Magnetics, **54**(3), article no. 8000504 (2018)
21. Yang, S. H., Kiang, J. F.: Optimization of sparse linear arrays using harmony search algorithms. IEEE Trans. Ant. Prop., **63**(11), pp 4732–4738 (2015)

ICCS Camera Ready Version 2022
To cite this paper please use the final published version:
DOI: 10.1007/978-3-031-08757-8_22

22. Zhang, Z., Cheng, Q. S., Chen, H., Jiang, F.: An efficient hybrid sampling method for neural network-based microwave component modeling and optimization. IEEE Microwave Wireless Comp. Lett., **30**(7), pp. 625–62 (2020)
23. Van Nechel, E., Ferranti, F., Rolain, Y., Lataire., J.: Model-driven design of microwave filters based on scalable circuit models. IEEE Trans. Microwave Theory Techn., **66**(10), pp. 4390–4396 (2018)
24. Li, Y., Xiao, S., Rotaru, M., Sykulski, J. K.: A dual kriging approach with improved points selection algorithm for memory efficient surrogate optimization in electromagnetics. IEEE Trans. Magn., **52**(3), pp. 1–4, Art no. 7000504 (2016)
25. Jacobs, J. P.: Characterization by Gaussian processes of finite substrate size effects on gain patterns of microstrip antennas. IET Microwaves Ant. Prop., **10**(11), pp. 1189–1195 (2016)
26. Ogut, M., Bosch-Lluis, X., Reising, S. C.: A deep learning approach for microwave and millimeter-wave radiometer calibration. IEEE Trans. Geoscience Remote Sens., **57**(8), pp. 5344–5355 (2019)
27. Lim, D. K., Yi, K. P., Jung, S. Y., Jung, H. K., Ro, J. S.: Optimal design of an interior permanent magnet synchronous motor by using a new surrogate-assisted multi-objective optimization. IEEE Trans. Magn., **51**(11), pp. 1–4, Art. no. 8207504 (2015)
28. Taran, N., Ionel, D. M., Dorrell, D. G.: Two-level surrogate-assisted differential evolution multi-objective optimization of electric machines using 3-D FEA. IEEE Trans. Magn., **54**(11), pp. 1–5, Art. no. 8107605 (2018)
29. Koziel, S., Pietrenko-Dabrowska, A., Performance-driven surrogate modeling of high-frequency structures, New York, NY, USA: Springer (2020)
30. Koziel, S.: Low-cost data-driven surrogate modeling of antenna structures by constrained sampling. IEEE Antennas Wireless Prop. Lett., **16**, pp. 461–464 (2017)
31. Pietrenko-Dabrowska, A., Koziel, S.: Antenna modeling using variable-fidelity EM simulations and constrained co-kriging. IEEE Access, **8**(1), pp. 91048–91056 (2020)
32. Koziel, S.: Fast simulation-driven antenna design using response-feature surrogates. Int. J. RF & Micr. CAE, **25**(5), pp. 394–402 (2015)
33. Koziel, S., Pietrenko-Dabrowska, A.: Expedited feature-based quasi-global optimization of multi-band antennas with Jacobian variability tracking. IEEE Access, **8**, pp. 83907–83915 (2020)
34. Koziel, S., Bandler, J. W.: Reliable microwave modeling by means of variable-fidelity response features. IEEE Trans. Microwave Theory Tech., **63**(12), pp. 4247–4254, (2015)
35. Pietrenko-Dabrowska, A. & Koziel, S.: Fast design closure of compact microwave components by means of feature-based metamodels. Electronic*s*, **10**, 10 (2021).
36. Conn, A. R., Gould, N. I. M. & Toint, P. L.: Trust Region Methods, MPS-SIAM Series on Optimization, Philadelphia, PA, USA: SIAM (2000).
37. Phani Kumar, K. V. & Karthikeyan, S. S.: A novel design of ratrace coupler using defected microstrip structure and folding technique. IEEE Applied Electromagnetics Conf. (AEMC), Bhubaneswar, India, pp. 1–2 (2013).
38. Lin, Z. & Chu, Q. -X.: A novel approach to the design of dual-band power divider with variable power dividing ratio based on coupled-lines. Prog. Electromagn. Res. **103**, pp. 271–284 (2010).
39. Kennedy, J. & Eberhart, R. C.: Swarm Intelligence, San Francisco, CA, USA, Morgan Kaufmann (2001).

ICCS Camera Ready Version 2022
To cite this paper please use the final published version:
DOI: 10.1007/978-3-031-08757-8_22